

Geometric Errors of the Pulsed-Wave Doppler Flow Method in Quantifying Degenerative Mitral Valve Regurgitation: A Three-dimensional Echocardiography Study

Ben Ren, Lotte E. de Groot-de Laat, Jackie McGhie, Wim B. Vletter, Folkert J. ten Cate and Marcel L. Geleijnse.

J Am Soc Echocardiogr 2013;26(3):261-69

ABSTRACT

Aim

The aim of this study was to estimate geometric errors made by the two-dimensional (2D) transthoracic echocardiographic (TTE) pulsed-wave Doppler flow (PWDF) method in calculating regurgitant volume (RVol) and effective regurgitant orifice area (EROA) in degenerative mitral regurgitation (MR) by comparison with the three-dimensional (3D) transesophageal echocardiographic (TEE) PWDF method.

Methods

RVol and EROA were calculated in 22 patients with degenerative MR using the conventional 2D TTE PWDF method on the basis of monoplanar dimensions and a circular geometric assumption of the crosssectional areas (CSAs) of the mitral annulus (MA) and the left ventricular outflow tract (LVOT) and the 3D TEE PWDF method, in which the CSAs of the MA and LVOT were measured directly in “en face” views. Diameters of the MA and LVOT were also measured in similar views as with TTE imaging in 3D TEE data sets.

Results

Both the MA and LVOT were oval. Mean MA diameters were 41 ± 4 mm (3D TEE major axis), 31 ± 4 mm (3D TEE minor axis), 39 ± 5 mm (2D TTE imaging), and 38 ± 5 mm (2D TEE imaging). Mean LVOT diameters were 29 ± 4 mm (3D TEE major axis), 21 ± 2 mm (3D TEE minor axis), 22 ± 2 mm (2D TTE imaging), and 23 ± 2 mm (2D TEE imaging). Compared with 3D TEE measurements, mitral annular CSA was overestimated by $13 \pm 12\%$ on 2D TTE imaging and by $7 \pm 14\%$ on 2D TEE imaging, while LVOT CSA was underestimated by $23 \pm 10\%$ and $17 \pm 10\%$, respectively. Mean values of RVol were 95 ± 43 mL (3D TEE PWDF), 137 ± 56 mL (2D TTE PWDF), 120 ± 45 mL (2D TEE PWDF), and 111 ± 49 mL (flow convergence). Mean EROAs were 69 ± 34 mm² (3D TEE PWDF), 98 ± 45 mm² (2D TTE PWDF), 88 ± 42 mm² (2D TEE PWDF), and 79 ± 36 mm² (flow convergence). Observer variability for 3D TEE imaging was better than for 2D imaging.

Conclusion

The 2D TTE PWDF method overestimates mitral RVol and EROA significantly because monoplanar 2D measurements represent mitral annular major-axis diameter and LVOT minor-axis diameter, and assumed circular CSAs of the MA and LVOT are oval.

INTRODUCTION

Quantification of mitral regurgitation (MR) is essential to determine the severity of MR and clinical outcomes^{1,2}. The two most used quantitative parameters are regurgitant volume (RVol) and effective regurgitant orifice area (EROA), which may be calculated by the flow convergence method and the pulsed-wave Doppler flow (PWDF) method as previously recommended^{1,3}. However, both of these methods suffer from geometric limitations of two-dimensional (2D) echocardiography. The flow convergence method potentially underestimates RVol and EROA in functional MR, because the shape of the flow convergence zone may be elliptic instead of hemispheric in this situation^{4,11}. In the PWDF method, important geometric errors are made in calculating the cross-sectional areas (CSAs) of the mitral annulus (MA) and left ventricular outflow tract (LVOT), because of the monoplanar measurements and geometric assumption¹². In this study, we sought to ascertain the geometric errors made by the traditional 2D transthoracic echocardiographic (TTE) PWDF method in calculating RVol and EROA in patients with degenerative MR, by comparison with the three-dimensional (3D) transesophageal echocardiographic (TEE) PWDF method. Using the latter method, the CSAs of the MA and LVOT were measured directly in state-of-the-art “en face” views on 3D TEE imaging.

METHODS

Study Population

From November 2009 to September 2011, we prospectively enrolled 96 consecutive patients referred to our center for potential mitral valve (MV) repair who had undergone baseline TTE and TEE examinations. In the present study, we included patients with (1) degenerative MR according to preoperative TTE findings, (2) P2 scallop prolapse confirmed by both 3D TEE examination and surgery, and (3) good 3D image quality, with complete regions of interest and without stitching artifacts. The exclusion criteria were (1) MR due to other etiologies or mechanisms (e.g., endocarditis, functional MR; $n = 39$), (2)

prolapse of other scallops ($n = 19$), (3) a severely calcified MA ($n = 11$), (4) more than trivial aortic valve regurgitation ($n = 3$), and (5) poor general image quality ($n = 2$). Eventually, 22 patients (12 men; mean age, 64 ± 10 years) were included in the study. The protocols were approved by the institutional review board, and informed consent was obtained from all patients.

PWDF Method

2D TTE Measurements. Two-dimensional TTE imaging was performed using the iE33 ultrasound system (Philips Medical Systems, Best, The Netherlands) with the S5-1 trans-

ducer. The pulsed-wave Doppler sample was carefully placed as parallel as possible (angle $< 20^\circ$) to the blood flow in the apical four-chamber and three-chamber views to obtain the Doppler spectral profiles of the MA and LVOT¹³. The mitral annular diameter was measured between the inner edges of the base of posterior and anterior leaflets in early to mid diastole at maximal MV opening in the apical four-chamber view; the LVOT diameter was measured just below the aortic valve in early to mid systole in the parasternal long-axis view^{3,13}. Both diameters were measured at the level at which the volume sample had been placed. The modal velocity profile on Doppler recordings was traced to obtain the velocity-time integral (VTI) (Figure 1). The regurgitant VTI was averaged from measurements in the apical four-chamber and three-chamber views. All measurements were averaged over three cardiac cycles.

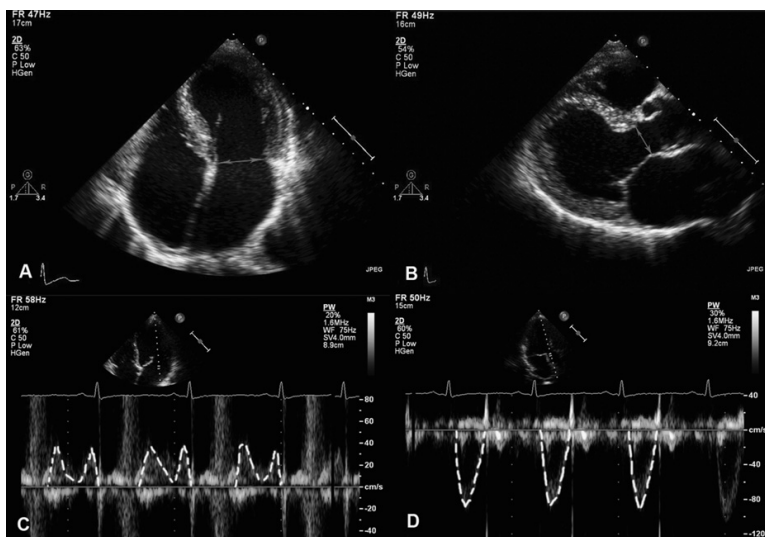


Figure 1. Measurements of the 2D TTE PWDF method. (A) The diameter of the MA was measured between the inner edges of the base of the posterior and anterior leaflets in early to mid diastole at the maximal opening of the MV (two to three frames after the MV opened) in the apical four-chamber view. (B) The diameter of the LVOT was measured just below the aortic valve in early to mid systole in the parasternal long-axis view. (C) Mitral annular inflow pulsed-wave Doppler was traced to obtain the VTI of mitral inflow. (D) LVOT pulsed-wave Doppler was traced to obtain the VTI of ventricular outflow.

3D TEE Measurements. Three-dimensional TEE imaging was performed using the iE33 ultrasound system with the X7-2t matrix-array transducer. Electrocardiographically gated full-volume data sets (built from seven subvolumes) were acquired at the midesophageal level during breath-hold with the ultrasound focus on the MV in the four-chamber view and on the LVOT in the long-axis view. Care was taken to include the complete mitral annular and LVOT circumferences throughout the acquisition. Each full-volume data set

was digitally stored and exported to QLAB 8.0 3DQ software (Philips Medical Systems) for offline analysis. The en face views of the MA and LVOT were revealed at time points during the cardiac cycle similar as for the 2D TTE measurements and adjusted to the level at which the pulsed-wave Doppler volume sample had been placed in the 2D TTE examinations. Subsequently, the inner border of the cross-sectional planes of the MA and LVOT as well as the major-axis and minor-axis diameters were measured (Figure 2).

2D TEE Measurements. By adjusting the orthogonal multiplanar reconstruction views of the 3D TEE data sets, the diameter of the MA was measured in the four-chamber view in early to mid diastole at the maximal opening of the MV, and that of the LVOT was measured in early systole in the long-axis view (Figure 2). Both diameters were measured at the level at which the volume sample had been placed. Using the same VTI_{MR} , VTI_{MA} , and VTI_{LVOT} values obtained during the 2D TTE examinations, the 2D TTE, 3D TEE, and 2D TEE measurements of the diameters or CSAs were used in the following formulas to calculate the RVol and EROA:

$$RVol = SV_{MA} - SV_{LVOT} = \pi r_{MA}^2 \times VTI_{MA} - \pi r_{LVOT}^2 \times VTI_{LVOT};$$

and

$$EROA = RVol / VTI_{MR};$$

where r is the radius and SV is the stroke volume.

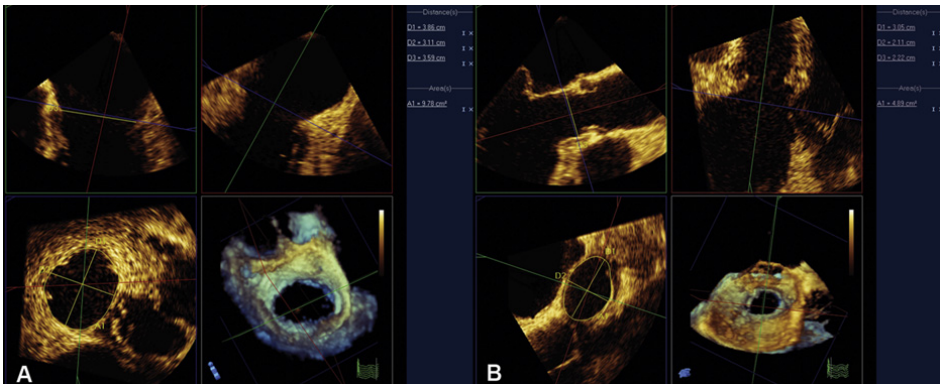


Figure 2.

Measurements of the 3D and 2D TEE PWDF methods. The 3D TEE data sets were displayed as three orthogonal images of the MA (A) and LVOT (B), and the visualization of the entire structures was optimized by adjusting the reference planes (the *green, red, and blue planes*). The blue planes showed the en face views of the MA and LVOT, in which the inner border of the CSAs of the MA and LVOT were traced manually and the CSAs and major and minor diameters were measured directly. The green plane (A) was adjusted to the four-chamber view and the mitral annular diameter was measured; the green plane (B) was adjusted to the long-axis view and the LVOT diameter was measured. All measurements were performed at the level at which the sample volume of pulsed-wave Doppler had been placed in the 2D TTE examinations.

Flow Convergence Method

The flow convergence of MR was shown in a zoomed view of color flow Doppler aliasing at the Nyquist velocity limit (30–40 cm/sec) in the apical four-chamber and three-chamber views. The selected cine loop was reviewed stepwise, and a clearly defined mid to late systolic maximal flow convergence zone was measured from the zenith to the regurgitant orifice. The averaged values measured in both views were used to calculate the RVol and EROA using the following formulas:

$$\text{EROA} = 2\pi r^2 \times V_a / PkV_{\text{Regurg}}$$

and

$$\text{RVol} = \text{EROA} \times \text{VTI}_{\text{MR}}$$

where r is the radius of the flow convergence, V_a is the aliasing velocity, and PkV_{Regurg} is the peak velocity of MR.

Vena Contracta Width

The vena contracta width of the MR jet was measured at the narrowest portion of the regurgitant jet in zoom mode with an adapted Nyquist limit (59.3 cm/sec) and averaged from the measurements in the four-chamber and three-chamber views.

Statistical analysis

All values are expressed as median (range) or as mean \pm SD. One-factorial repeated-measures analysis of variance or Friedman's analysis of variance was used to compare the diameters, CSAs, SVs, RVols, and EROAs calculated using the different methods. When differences were found, any two methods were compared using the paired t test or Wilcoxon's signed-rank test with Bonferroni's correction. Linear regression analysis was used to assess the correlation of variables of interest. Agreement between methods was assessed using Bland-Altman method, in which differences were plotted against the means of measurements. Interobserver and intraobserver variabilities were tested by analyzing 2D and 3D images by two blinded observers (B.R., L.G.L.) and by the same observer (B.R.) at two difference times. The results were analyzed by the relative difference (expressed as the absolute difference divided by the mean) and Bland-Altman method.

RESULTS

Baseline Characteristics of the Patient Population in the Echocardiographic Studies

All patients included underwent MV repair. The baseline TTE examination was performed to ascertain the severity of MR, and the TEE examination performed on the same day was performed to determine the exact mechanism of MR and guide the selection of the cardiac surgeon. However, the preoperative TEE examination was declined or unsuccessful in eight patients, and in one patient, image quality was inferior because of poor general image quality and 3D stitching artifacts. For these nine patients, intraoperative TEE imaging under general anesthesia was chosen as the baseline TEE study. The intraoperative TEE examination was performed within 24 hours of the baseline TTE examination in three patients and 6 to 35 days after the baseline TTE examination in six patients. Of the 13 patients who underwent both baseline TTE and TEE imaging in the outpatient clinic, nine also underwent intraoperative TEE imaging. The time period between the preoperative TEE study and the intraoperative TEE study was 1 to 32 days. Although the hemodynamic characteristics of these nine patients changed significantly, the shapes and sizes of the MA and LVOT remained relatively constant (Table 1).

Table 1. Comparisons of the patients' hemodynamic characteristics and mitral annular and LVOT morphologies in the preoperative and intraoperative TEE examinations ($n = 9$)

Variable	Preoperative TEE imaging	Intraoperative TEE imaging
Heart rate (beats/min)	97 (71-123)	68 (48-99)
Bloodpressure (mmHg)		
Systolic	140 (110-163)	105 (80-125)
Diastolic	80 (60-88)	50 (40-75)
MA		
Major-axis/minor-axis diameter ratio	1.3 (1.0-1.6)	1.4 (1.1-1.5)
CSA (mm ²)	1,058 (840-1,542)	1,105 (747-1,788)
LVOT		
Major-axis/minor-axis diameter ratio	1.4 (1.2-1.7)	1.4 (1.1-1.5)
CSA (mm ²)	497 (443-723)	548 (424-630)

Data are expressed as median (range)

Comparison of the 2D and 3D Dimensions and CSAs of the MA and LVOT

The frame rate of the 2D data sets and volume rate of the 3D data sets were not different (49.6 ± 6 frames/sec vs 46 ± 8 volumes/sec). As shown in Table 2, the 2D TTE and 2D TEE diameters of the MA and LVOT were not significantly different from each other. Both the MA and LVOT were oval in the 3D en face views, with a significant difference between the major-axis and minor-axis diameters ($P < .001$ for both). The major-axis/minor-axis diameter ratio of the MA was 1.3 ± 0.2 , and that of the LVOT was 1.4 ± 0.2 . The 2D diameters

of the MA and LVOT were significantly different from both the major- axis and minor-axis diameters ($P < .05$ for all). The CSAs of the MA and LVOT calculated from 2D TTE and 2D TEE diameters were similar. For the CSA of the MA, the 2D TTE measurements were significantly different from the 3D TEE direct measurement ($P < .001$) and overestimated the CSA by $13 \pm 12\%$; although the 2D TEE measurements were not significantly different from the 3D TEE measurements, the CSA was still overestimated by $7 \pm 14\%$. For the CSA of the LVOT, both 2D TTE and 2D TEE measurements were significantly different from the 3D TEE direct measurements ($P < .001$ for both), and the CSAs were underestimated by $23 \pm 10\%$ by the 2D TTE measurements and $17 \pm 10\%$ by the 2D TEE measurements.

Table 2. The diameters and CSAs of the MA and LVOT in degenerative MR obtained with the 2D and 3D measurements

Structure	Diameter (mm)				CSA (mm ²)		
	2D measurements		3D TEE measurements		2D measurements		3D TEE measurements
	TTE imaging	TEE imaging	Major axis	Minor axis	TTE imaging	TEE imaging	
MA	$39 \pm 5^{*\dagger}$	$38 \pm 5^\ddagger$	$41 \pm 4^\S$	31 ± 4	$1,185 \pm 304^{*\#}$	$1,117 \pm 254^\S$	$1,050 \pm 247$
LVOT	$22 \pm 2^{*\dagger}$	$23 \pm 2^\ddagger$	$29 \pm 4^\S$	21 ± 2	$391 \pm 73^{*\#}$	$426 \pm 80^\S$	517 ± 110

* $P = NS$ for 2D TTE versus 2D TEE measurements.

† $P < .05$ for 2D TTE versus 3D TEE measurements.

‡ $P < .001$ for 2D TEE versus 3D TEE measurements.

§ $P < .001$ for 3D TEE major versus minor axis measurements.

$P < .001$ for 2D TTE versus 3D TEE measurements.

†† $P = NS$ for 2D TEE versus 3D TEE measurements.

Comparison of Mitral RVol and EROA by the 2D and 3D PWDF and Flow Convergence Methods

As a result of the differences in CSAs obtained by 2D and 3D measurements, the SV at the mitral annular level was overestimated by $13 \pm 12\%$ by the 2D TTE measurements and by $7 \pm 14\%$ by the 2D TEE measurements, while the SV at the LVOT level was underestimated by $23 \pm 10\%$ by the 2D TTE measurements and by $17 \pm 10\%$ by the 2D TEE measurements. The RVol and EROA obtained by the 3D TEE PWDF method were significantly smaller than those calculated by the 2D PWDF methods ($P < .001$ for all; Table 3). Compared with the 3D TEE measurements, RVol and EROA were overestimated by $54 \pm 39\%$ by the 2D TTE PWDF method and by $39 \pm 40\%$ by the 2D TEE PWDF method.

Compared with the flow convergence method, the RVols obtained by the 3D PWDF methods correlated better with the RVols obtained using the flow convergence method than the 2D PWDF methods did (2D TTE PWDF vs flow convergence, $r = 0.91$; 2D TEE PWDF vs flow convergence, $r = 0.72$; 3D PWDF vs flow convergence, $r = 0.94$; Figure 3). Com-

Table 3. SVs at the level of the MA and LVOT and mitral RVol and EROA obtained by the flow convergence and 2D and 3D PWDF methods

Variable	Flow convergence method	PWDF method		
		2D TTE imaging	2D TEE imaging	3D TEE imaging
SV (mL)				
MA	-	198 ± 55 ^{*,†}	186 ± 44 [‡]	175 ± 42
LVOT	-	61 ± 21 ^{*,†}	66 ± 20 [§]	80 ± 23
RVol (mL)	111 ± 49	137 ± 56 ^{†,‡,¶}	120 ± 45 ^{§,#}	95 ± 43 ^{**}
EROA (mm ²)	79 ± 36	98 ± 45 ^{*,†,¶}	880 ± 42 ^{§,#}	69 ± 34 ^{**}

**P* = NS for 2D TTE versus 2D TEE PWDF method.

†*P* < .001 for 2D TTE versus 3D TEE PWDF method.

‡*P* = NS for 2D TEE versus 3D TEE PWDF method.

§*P* < .001 for 2D TEE versus 3D TEE PWDF method.

¶*P* < .05 for 2D TTE versus 2D TEE PWDF method.

††*P* < .001 for 2D TTE PWDF versus flow convergence method.

#*P* = NS for 2D TEE PWDF versus flow convergence method.

***P* < .05 for 3D TEE PWDF versus flow convergence method.

parisons with the flow convergence method revealed that RVol was overestimated by 24 ± 23% by the 2D TTE PWDF method (137 ± 56 vs 111 ± 49 mL, *P* < .001) and by 14 ± 40% by the 2D TEE PWDF method (120 ± 45 vs 111 ± 49 mL) but underestimated by 17 ± 17% by the 3D TEE PWDF method (95 ± 43 vs 111 ± 49 mL, *P* < .05). A very similar pattern was found for EROA. Here too, the EROAs obtained by the 3D PWDF method correlated better with those obtained using the flow convergence method than the 2D PWDF methods did (2D TTE PWDF vs flow convergence, *r* = 0.92; 2D TEE PWDF vs flow convergence, *r* = 0.76; 3D PWDF vs flow convergence, *r* = 0.95; Figure 3). The magnitude of the overestimation and underestimation by comparison with the flow convergence method was the same as for RVol: the EROA was overestimated by 24 ± 23% by the 2D TTE PWDF method (98 ± 45 vs 79 ± 36 mm², *P* < .001) and by 14 ± 40% by the 2D TEE PWDF method (88 ± 42 vs 79 ± 36 mm²) but underestimated by 17 ± 17% by the 3D PWDF method (69 ± 34 vs 79 ± 36 mm², *P* < .05).

Bland-Altman analysis plots for agreement of the RVol and EROA between the PWDF methods and flow convergence method are also depicted in Figure 3. For RVol, the bias ± 2 standard deviations was 26 ± 48 mL (2D TTE PWDF vs flow convergence), 9 ± 71 mL (2D TEE PWDF vs flow convergence), and 16 ± 34 mL (3D TEE PWDF vs flow

convergence). For EROA, the bias ± 2 standard deviations was 20 ± 38 mm² (2D TTE PWDF vs flow convergence), 9 ± 56 mm² (2D TEE PWDF vs flow convergence), and 10 ± 23 mm² (3D TEE PWDF vs flow convergence). There was smaller bias and tighter limits of agreement between the 3D TEE PWDF and flow convergence methods than between the 2D PWDF and flow convergence methods.

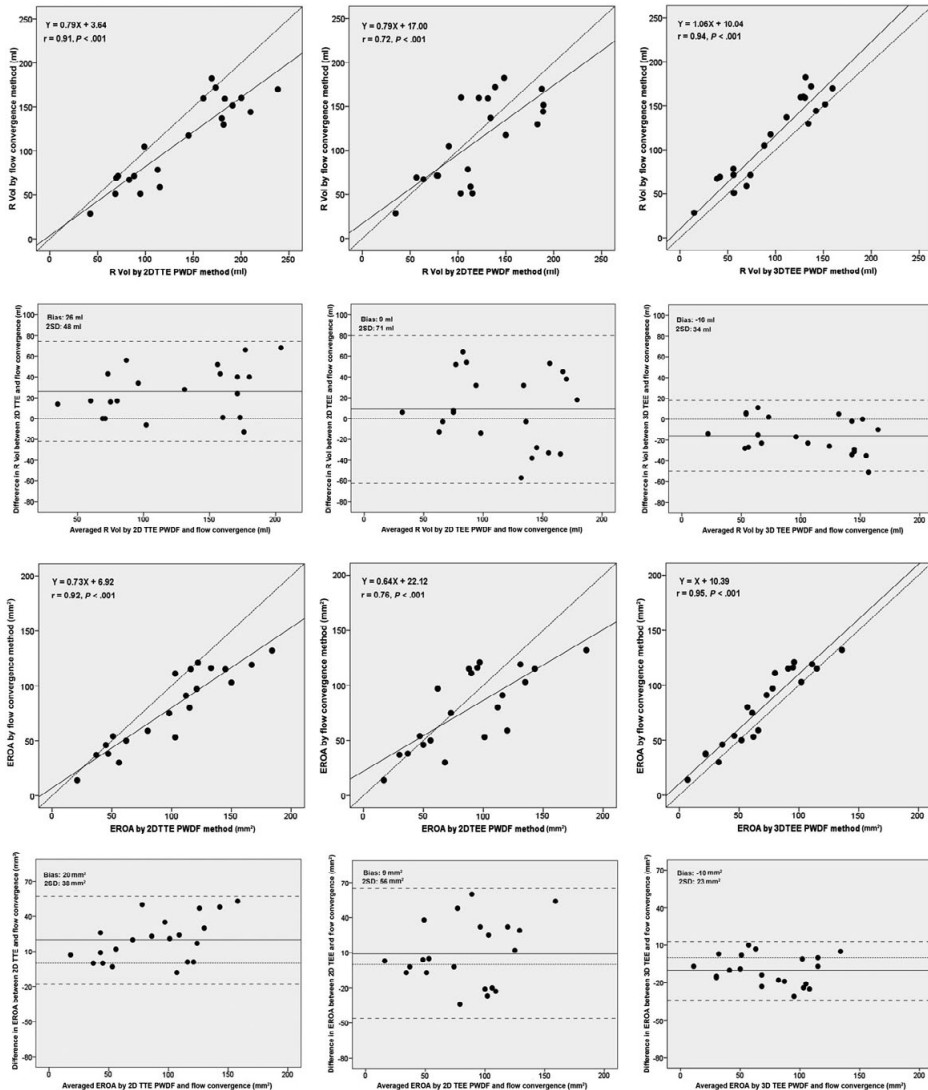


Figure 3.

Linear regression and Bland-Altman analysis comparing the mitral RVol and EROA by the 2D TTE (*left column*), 2D TEE (*middle column*), and 3D TEE (*right column*) PWDF methods, with respective values by the flow convergence method.

Categorizations of MR Severity according to Different Methods

The MR severity of the patients included was categorized according to the RVol and EROA calculated by the 2D TTE, 2D TEE, 3D TEE PWDF, and flow convergence methods and vena contracta width on the basis of the American Society of Echocardiography’s recommendations for evaluation of the severity of native valvular regurgitation using 2D and

Doppler echocardiography¹. The severity of MR was different in five patients (Table 4) and the same for the other 17 patients.

Table 4. Categorization of MR severity in patients with discrepancies in MR severity using different methods ($n = 5$)

Patient	2D TTE PWDF	2D TEE PWDF	3D TEE PWDF	Flow convergence	Vena contracta
1	Severe	Severe	Moderate	Severe	Moderate
2	Severe	Severe	Moderate to severe	Moderate to severe	Moderate
3	Severe	Severe	Moderate to severe	Severe	Severe
4	Severe	Severe	Moderate to severe	Moderate to severe	Moderate
5	Severe	Severe	Moderate to severe	Severe	Severe

Intraobserver and Interobserver Variabilities of 2D and 3D Measurements

For all measurements, intraobserver and interobserver variabilities of the 3D TEE PWDF method was better in terms of the relative difference and limits of agreement (Table 5).

Table 5. Intraobserver and interobserver variabilities of the 2D and 3D PWDF methods in measurements of the diameters and CSAs of the MA and LVOT and mitral RVol and EROA

Variable	Intraobserver variability			Interobserver variability		
	2D TTE imaging	2D TEE imaging	3D TEE imaging	2D TTE imaging	2D TEE imaging	3D TEE imaging
Relative difference (%)						
Mitral annular diameter	6 ± 8	3 ± 2	-	13 ± 12	7 ± 8	-
Mitral annular CSA	12 ± 16	6 ± 4	10 ± 9	21 ± 20	14 ± 16	16 ± 11
LVOT diameter	6 ± 6	4 ± 3	-	8 ± 7	8 ± 6	-
LVOT CSA	11 ± 11	8 ± 6	6 ± 4	16 ± 13	16 ± 12	15 ± 9
RVol	24 ± 31	19 ± 18	22 ± 21	46 ± 61	27 ± 31	33 ± 26
EROA	24 ± 31	19 ± 18	22 ± 21	46 ± 61	27 ± 31	33 ± 26
Bias ± limits of agreement						
Mitral annular diameter (mm)	-1 ± 6	0 ± 3	-	-3 ± 8	1 ± 7	-
Mitral annular CSA (mm ²)	-21 ± 306	3 ± 174	-39 ± 271	-112 ± 325	55 ± 401	93 ± 228
LVOT diameter (mm)	-1 ± 3	0 ± 2	-	-1 ± 4	1 ± 4	-
LVOT CSA (mm ²)	-24 ± 106	7 ± 90	-13 ± 68	-37 ± 117	52 ± 122	-60 ± 114
RVol (mL)	1 ± 57	0 ± 30	-4 ± 49	-13 ± 91	12 ± 78	27 ± 73
EROA (mm ²)	1 ± 43	1 ± 23	-1 ± 36	-11 ± 69	10 ± 57	18 ± 50

Relative difference = absolute difference/mean × 100%; bias = mean of differences; limits of agreement = 2 standard deviations.

DISCUSSION

The main finding of this study is that compared with the 3D TEE PWDF method, the traditional 2D TTE PWDF method overestimated mitral RVol and EROA significantly. The overestimates were caused by the oversimplified 2D measurements and the geometric assumption of the CSAs of the MA and LVOT, which led to the CSA and SV being overestimated at the mitral annular level and underestimated at the LVOT level.

Measurements of the CSAs of the MA and LVOT Using the PWDF Method

In the 2D TTE PWDF method, the preferred sites to calculate the SVs are the MA and LVOT, so precise measurements of the MA and LVOT dimensions are crucial. Conventionally, the mitral annular dimension is measured in the apical four-chamber view and the LVOT dimension in the parasternal long-axis view^{1,3,13}. These measurements have important limitations and lead to errors in calculating CSAs, because variable and unpredictable monoplanar cross-sections are made and circular geometry of the orifices is assumed. In reality, the CSAs of both the MA and LVOT are oval, with the major and minor diameters¹⁴⁻¹⁸. In this study, the 2D mitral annular diameters approached the 3D major-axis diameters, and the 2D LVOT diameters were close to the 3D minor-axis diameters (Figure 4), which is consistent with previous findings¹⁶⁻¹⁹. The monoplanar measurements and false geometric assumption are important sources of error in measuring the mitral annular and LVOT dimensions using the 2D PWDF method. The error is further magnified because the diameter (radius) values are squared in the geometric assumption formula. Due to the important geometric errors, the CSA of the MA and corresponding SV were overestimated by $13 \pm 12\%$ and the CSA of the LVOT and corresponding SV were underestimated by $23 \pm 10\%$ by the 2D TTE measurements, compared with the 3D CSAs measured directly in the en face views of the MA and LVOT at the level at which the velocity profiles had been recorded.

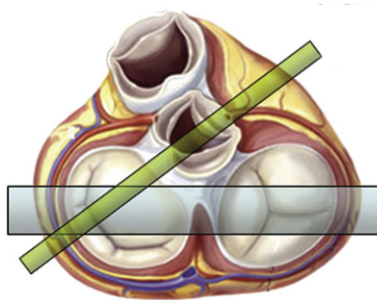


Figure 4.

Orientations of the traditional 2D echocardiographic imaging planes of the MA (apical four-chamber view) and LVOT (parasternal long-axis view).

The spatial resolution of the TEE images is better than that of the TTE images, thus allowing a clearer identification of anatomic landmarks (e.g., the hinge points of the mitral leaflets). The difference in CSAs between 2D TEE and 3D TEE measurements was smaller (2D TEE imaging overestimated mitral annular CSA by $7 \pm 14\%$ and underestimated LVOT CSA by $17 \pm 10\%$). The errors, however, especially for the CSA of the LVOT, were still considerable. Moreover, the errors of both 2D TTE and TEE measurements in calculating the SVs were in different directions (i.e., overestimation at the mitral annular level and underestimation at the LVOT level), so the consequent impact in calculating RVol and EROA was even more significant, with an overestimate of $54 \pm 39\%$ by the 2D TTE PWDF method and $39 \pm 40\%$ by the 2D TEE PWDF method.

To measure the cardiac structures using the echocardiographic approaches, especially the CSAs of the MA and LVOT, we believe that 3D echocardiography improves the accuracy of measurements greatly because the structures of interest can be revealed in the en face views and measured directly without the geometric assumption used in the 2D echocardiographic method. Additionally, the transesophageal imaging approach contributes to improved accuracy because the cardiac structures (e.g., the MA) lie in the near field of the ultrasound field, resulting in better spatial resolution. We assume that the observer variability of 3D TTE measurements would be higher than those of 3D TEE measurements because of insufficient spatial resolution of the 3D TTE data sets.

The 2D and 3D PWDF Methods in Calculating Mitral RVol and EROA Compared with the Flow Convergence Method

The flow convergence method is one of the methods recommended for quantifying degenerative MR, because the isovelocity surface is usually hemispheric^{10,20-22}. The RVol and EROA calculated by the 3D TEE PWDF method had better correlations and agreement with the flow convergence method than the 2D PWDF methods did. The 2D PWDF methods overestimated the RVol and EROA compared with both the 3D TEE PWDF and flow convergence methods. Surprisingly, the RVol and EROA calculated by the 3D TEE PWDF method were smaller than those obtained by the flow convergence method. The probable reason is that the flow convergence method overestimates the true RVol and EROA, as it estimates regurgitant flow from the “maximal” flow rate and thus overestimates the mean flow rate, especially in the situation of a dynamic orifice area change during systole seen in degenerative MR^{23,24}. In our study, the flow convergence was measured in late systole in six cases because of the late systolic enhancement of MR due to prolapsed leaflets (Figure 5A). This overestimates the mean EROA because the timing of the flow convergence measurement and the peak velocity of the regurgitation is not synchronized. Additionally, the density of the continuous-wave Doppler profile of MR in these cases was faint in early systole and became denser in late systole (Figure 5B), probably causing overestimation of the VTI of MR and thus further overestimation of RVol. Other physiologic and technical

factors can also substantially influence flow quantification by this approach; they include the regurgitant orifice motion, aliasing velocity, and ratio of the aliasing velocity to peak orifice velocity^{3,24}.

It is crucial to understand the etiology and mechanism of MR and underlying principles and limitations of the flow convergence method when using this method to quantify MR. The pitfalls of applying the flow convergence method to the situations of a nonhemispheric flow convergence zone and a dynamically changing regurgitant orifice have been highlighted by extensive in vitro and clinical studies^{4-11,23,25}. The major advantage of the PWDF method is the volumetric measures, whereby SV at the mitral annular level is measured in diastole and is thus not affected by the spatial or temporal homogeneity of MR in systole.

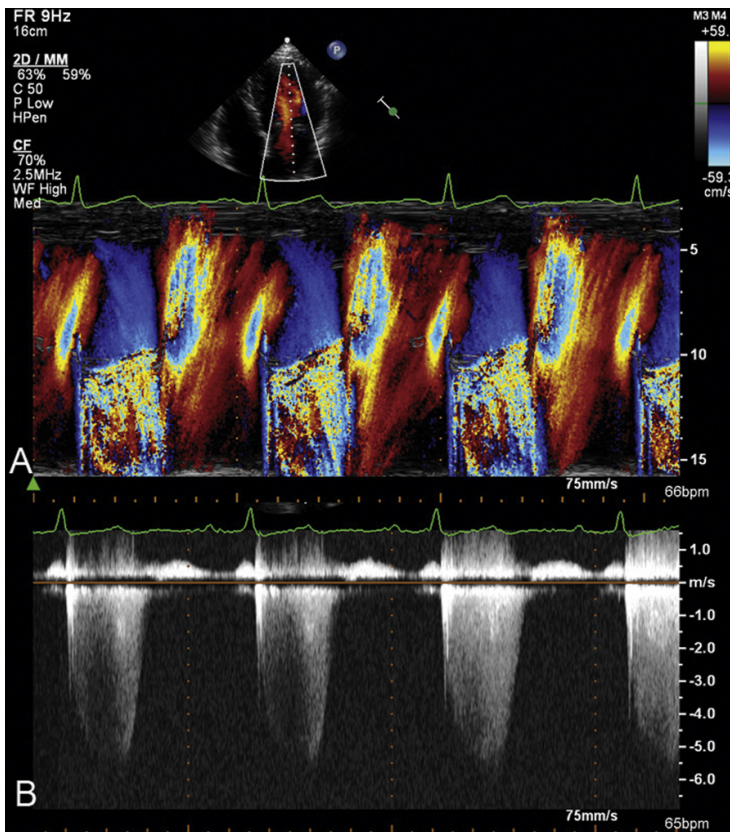


Figure 5.

The “late systolic enhancement” of MR due to a prolapsed P2 scallop. (A) Color M-mode echocardiography shows that the regurgitation increased progressively, with a maximum in late systole. (B) Continuous-wave Doppler echocardiography shows that the density of the profile was faint in early systole and became denser in late systole.

Discrepancies in Grading the Severity of MR according to Different Methods

In five patients, the categorization of MR severity was different according to different quantitative methods; more specifically, it was less severe according to the 3D TEE PWDF method. For patients 2 and 4 (Table 4), MR severity was probably overestimated by the 2D TTE PWDF method, which was confirmed by the 3D TEE PWDF method, flow convergence method, and vena contracta width. For patients 1 and 3, there was a late systolic enhancement of MR, so the severity was likely to be overestimated by the flow convergence method and vena contracta width as well. In only one patient, patient 5, there were mismatches of MR severity according to different methods. Because all five patients had been symptomatic, although MR severity was “less than severe” according to the 3D TEE PWDF method, clinical management was not changed, and all patients underwent MV repair. There is no clinical evidence that the five patients benefited less from MV repair.

Intraobserver and Interobserver Variabilities

The TEE PWDF methods were generally more reproducible than 2D TTE PWDF method, mainly because of the better spatial resolution of TEE imaging. Additionally, when the 3D TEE PWDF method was used, the relative differences and limits of agreement of the intraobserver and interobserver measurements for RVol and EROA were smaller than those in the 2D PWDF methods. As expected, the major cause of variability in PWDF methods was the measurements of the CSAs of the MA and LVOT. For the 2D and 3D PWDF methods, the variability resulted from the differences in choosing image frames and locating sampling planes for measurements. Although the intraobserver and interobserver variabilities of the 2D diameters of the MA and LVOT was relatively small, corresponding variability of the CSAs of the MA and LVOT was significantly higher because the 2D diameters (radii) are squared in the geometric assumption formula for CSA.

Limitations

A true gold standard for calculating RVol and EROA was absent in the present study. The flow convergence method was used as the reference method, but underlying assumptions of this method are not entirely valid in the situations of an eccentric regurgitant jet and a dynamic regurgitant orifice change during systole, as discussed previously. We believe that a nonechocardiographic imaging modality (e.g., cardiac magnetic resonance imaging) would be much more helpful in validating our findings.

Mitral regurgitant jets due to prolapsed leaflets usually direct eccentrically, and the flow convergence method is less accurate. In this study, most patients had isolated P2 scallop prolapse, and the flow convergence zones were visually smooth and measurable.

The sample size in this study was relatively small because only patients who had optimal available echocardiographic assessments of CSAs of the MA and LVOT by 3D TEE imag-

ing were included. Nevertheless, in all patients included, a consistent trend of overestimating mitral RVol and EROA using the 2D TTE PWDF method was obvious and therefore meaningful for clinical practice.

Because the MA and LVOT are dynamic structures, differences in timing of the measurements may produce different values. In this study, the 2D frame rate and 3D volume rate were comparable, and the time points of measurements were set approximately equal in the cardiac cycle. We assume that the acquisition depth during 3D TEE imaging, which was half that of the 2D acquisition, contributed most to the high volume rate of the 3D data sets.

Finally, in some cases, the Doppler sound beam was not perfectly parallel to the blood flow. However, small deviations ($<20^\circ$) in angle produce mild ($<10\%$) errors in velocity measurements, and these errors may be acceptable for low-velocity flows¹³.

CONCLUSION

The traditional 2D TTE PWDF method tends to overestimates mitral RVol and EROA because the 2D measurements are monoplanar, and it is assumed that the CSAs of the MA and LVOT are circular, which results in the SV being overestimated at the mitral annular level and underestimated at the LVOT level.

REFERENCES

1. Zoghbi WA, Enriquez-Sarano M, Foster E, Grayburn PA, Kraft CD, Levine RA, et al. Recommendations for evaluation of the severity of native valvular regurgitation with two-dimensional and Doppler echocardiography. *J Am Soc Echocardiogr* 2003;16:777-802.
2. Enriquez-Sarano M, Avierinos JF, Messika-Zeitoun D, Detaint D, Capps M, Nkomo V, et al. Quantitative determinants of the outcome of asymptomatic mitral regurgitation. *N Engl J Med* 2005;352:875-83.
3. Lancellotti P, Moura L, Pierard LA, Agricola E, Popescu BA, Tribouilloy C, et al. European Association of Echocardiography recommendations for the assessment of valvular regurgitation. Part 2: mitral and tricuspid regurgitation (native valve disease). *Eur J Echocardiogr* 2010;11:307-32.
4. Hopmeyer J, He S, Thorvig KM, McNeil E, Wilkerson PW, Levine RA, et al. Estimation of mitral regurgitation with a hemielliptic curve-fitting algorithm: in vitro experiments with native mitral valves. *J Am Soc Echocardiogr* 1998;11:322-31.
5. Hopmeyer J, Whitney E, Papp DA, Navathe MS, Levine RA, Kim YH, et al. Computational simulations of mitral regurgitation quantification using the flow convergence method: comparison of hemispheric and hemielliptic formulae. *Ann Biomed Eng* 1996;24:561-72.
6. Li X, Shiota T, Delabays A, Teien D, Zhou X, Sinclair B, et al. Flow convergence flow rates from 3-dimensional reconstruction of color Doppler flow maps for computing transvalvular regurgitant flows without geometric assumptions: an in vitro quantitative flow study. *J Am Soc Echocardiogr* 1999;12:1035-44.
7. Little SH, Igo SR, Pirat B, McCulloch M, Hartley CJ, Nose Y, et al. In vitro validation of real-time three-dimensional color Doppler echocardiography for direct measurement of proximal isovelocity surface area in mitral regurgitation. *Am J Cardiol* 2007;99:1440-7.
8. Matsumura Y, Saracino G, Sugioka K, Tran H, Greenberg NL, Wada N, et al. Determination of regurgitant orifice area with the use of a new three-dimensional flow convergence geometric assumption in functional mitral regurgitation. *J Am Soc Echocardiogr* 2008;21:1251-6.
9. Shiota T, Sinclair B, Ishii M, Zhou X, Ge S, Teien DE, et al. Three-dimensional reconstruction of color Doppler flow convergence regions and regurgitant jets: an in vitro quantitative study. *J Am Coll Cardiol* 1996;27: 1511-8.
10. Utsunomiya T, Ogawa T, Doshi R, Patel D, Quan M, Henry WL, et al. Doppler color flow "proximal isovelocity surface area" method for estimating volume flow rate: effects of orifice shape and machine factors. *J Am Coll Cardiol* 1991;17:1103-11.
11. Yosefy C, Levine RA, Solis J, Vaturi M, Handschumacher MD, Hung J. Proximal flow convergence region as assessed by real-time 3-dimensional echocardiography: challenging the hemispheric assumption. *J Am Soc Echocardiogr* 2007;20:389-96.
12. Little SH, Ben Zekry S, Lawrie GM, Zoghbi WA. Dynamic annular geometry and function in patients with mitral regurgitation: insight from three-dimensional annular tracking. *J Am Soc Echocardiogr* 2010;23:872-9.
13. Quinones MA, Otto CM, Stoddard M, Waggoner A, Zoghbi WA, Doppler Quantification Task Force of the Nomenclature and Standards Committee of the American Society of Echocardiography, et al. Recommendations for quantification of Doppler echocardiography: a report from the Doppler Quantification Task Force of the Nomenclature and Standards Committee of the American Society of Echocardiography. *J Am Soc Echocardiogr* 2002;15:167-84.

14. Anwar AM, Soliman OI, Nemes A, Germans T, Krenning BJ, Geleijnse ML, et al. Assessment of mitral annulus size and function by real-time 3-dimensional echocardiography in cardiomyopathy: comparison with magnetic resonance imaging. *J Am Soc Echocardiogr* 2007;20: 941-8.
15. Anwar AM, Soliman OI, ten Cate FJ, Nemes A, McGhie JS, Krenning BJ, et al. True mitral annulus diameter is underestimated by two-dimensional echocardiography as evidenced by real-time three-dimensional echocardiography and magnetic resonance imaging. *Int J Cardiovasc Imaging* 2007; 23:541-7.
16. Doddamani S, Bello R, Friedman MA, Banerjee A, Bowers JH Jr., Kim B, et al. Demonstration of left ventricular outflow tract eccentricity by real time 3D echocardiography: implications for the determination of aortic valve area. *Echocardiography* 2007;24:860-6.
17. Doddamani S, Grushko MJ, Makaryus AN, Jain VR, Bello R, Friedman MA, et al. Demonstration of left ventricular outflow tract eccentricity by 64-slice multi-detector CT. *Int J Cardiovasc Imaging* 2009;25:175-81.
18. Otani K, Takeuchi M, Kaku K, Sugeng L, Yoshitani H, Haruki N, et al. Assessment of the aortic root using real-time 3D transesophageal echocardiography. *Circ J* 2010;74:2649-57.
19. Foster GP, Dunn AK, Abraham S, Ahmadi N, Sarraf G. Accurate measurement of mitral annular dimensions by echocardiography: importance of correctly aligned imaging planes and anatomic landmarks. *J Am Soc Echocardiogr* 2009;22:458-63.
20. Okamoto M, Tsubokura T, Nakagawa H, Morichika N, Amioka H, Yamagata T, et al. The suction signal detected by color Doppler echocardiography in patients with mitral regurgitation: its clinical significance [article in Japanese]. *J Cardiol* 1988;18:739-46.
21. Rodriguez L, Anconina J, Flachskampf FA, Weyman AE, Levine RA, Thomas JD. Impact of finite orifice size on proximal flow convergence. Implications for Doppler quantification of valvular regurgitation. *Circ Res* 1992;70:923-30.
22. Utsunomiya T, Doshi R, Patel D, Mehta K, Nguyen D, Henry WL, et al. Calculation of volume flow rate by the proximal isovelocity surface area method: simplified approach using color Doppler zero baseline shift. *J Am Coll Cardiol* 1993;22:277-82.
23. Enriquez-Sarano M, Miller FA Jr., Hayes SN, Bailey KR, Tajik AJ, Seward JB. Effective mitral regurgitant orifice area: clinical use and pitfalls of the proximal isovelocity surface area method. *J Am Coll Cardiol* 1995;25:703-9.
24. Simpson IA, Shiota T, Gharib M, Sahn DJ. Current status of flow convergence for clinical applications: is it a leaning tower of "PISA"? *J Am Coll Cardiol* 1996;27:504-9.
25. Buck T, Plicht B, Kahlert P, Schenk IM, Hunold P, Erbel R. Effect of dynamic flow rate and orifice area on mitral regurgitant stroke volume quantification using the proximal isovelocity surface area method. *J Am Coll Cardiol* 2008;52:767-78.